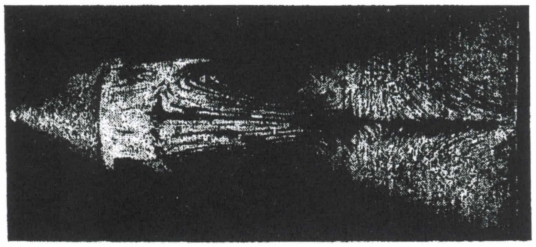

a) Leeward

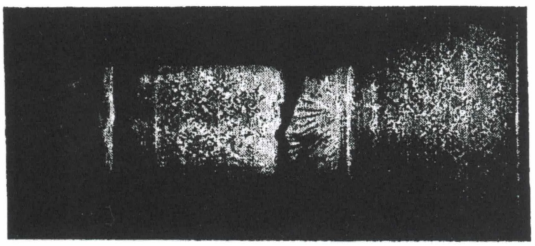

b) Profile

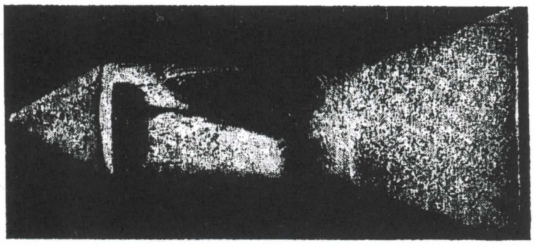

c) Windward

Fig. 4 China clay flow patterns; $\alpha = 4°$, M = 1.2, 2.0 caliber cylinder.

The flow photographs presented were selected for their ability to maintain their salient features after reduction. Previous experience[6] indicates that the boundary layer at separation is transitional for the 2.0 caliber cylinder (separation Reynolds number of 1.25×10^6 based on separation location aft of shoulder). However, for a longer cylinder where shadowgraph photographs indicate turbulent separation (separation Reynolds number = 2.36×10^6), similar vortex patterns are evident (Fig. 6).

These flow pictures indicate that serious reappraisal of current theoretical separated flow models may be in order since present models do not consider the circumferential communication effects revealed by the present investigation. Further experimental work is also warranted.

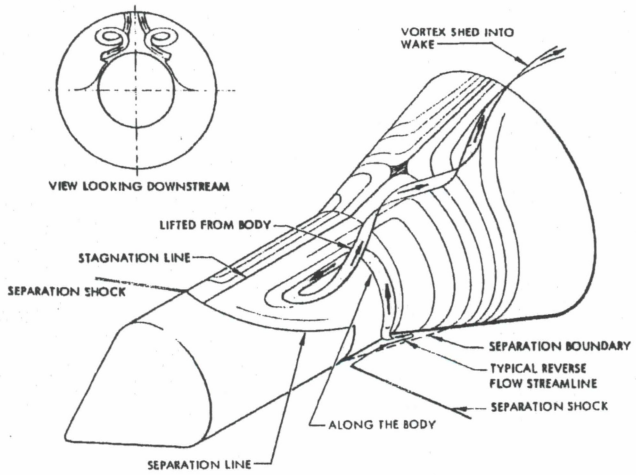

Fig. 5 Three-dimensional model.

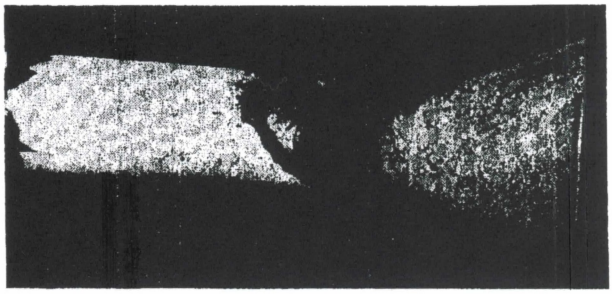

Fig. 6 China clay flow patterns; $\alpha = 4°$, M = 1.2, 3.5 caliber cylinder.

References

[1] Chapman, D. R., Kuehn, D. M., and Larson, H. K., "Investigation of Separated Flow in Supersonic and Subsonic Streams with Emphasis on the Effect of Transition," TN-3869, March 1957, NASA.

[2] Chevalier, H. L., private communication of currently unpublished data.

[3] Ginoux, T., "Experimental Evidence of Three-Dimensional Perturbations in the Reattachment of a Two-Dimensional Laminar Boundary Layer at M = 2.05," TN-1, 1958, Training Center for Experimental Aerodynamics, Belgium.

[4] Rosko, A. and Thomke, G. J., "Observations of Turbulent Reattachment Behind an Axisymmetric Downstream-Facing Step in Supersonic Flow," *AIAA Journal*, Vol. 4, No. 6, June 1966, pp. 975–980.

[5] Pope, A. and Goin, K. L., *High Speed Wind Tunnel Testing*, Wiley, New York, 1965.

[6] Guenther, R. A. and Reding, J. P., "Preliminary Experimental Investigation of Separated Flow Loads on Cone-Cylinder-Flare Bodies," L-87-67-1, Feb. 1967, Lockheed Missiles & Space Co., Sunnyvale, Calif.

Transonic Flow in Small Throat Radius of Curvature Nozzles

J. R. KLIEGEL* AND J. N. LEVINE†
Dynamic Science, a Division of Marshall Industries, Monrovia, Calif.

THE transonic flow region in convergent-divergent nozzles has been widely studied. The application of various expansion techniques to this problem has proven to be one of the more successful methods of analysis. Different investigators have employed various expansion techniques,[1–6] ranging from double power series expansions to small parameter expansions about the sonic condition. All of these methods are essentially the same, being perturbations about the one-dimensional flow solution. The deviation from one-dimensional flow is determined by the normalized throat wall radius of curvature R, the ratio of the throat wall radius of curvature R_w to the throat radius $r^*(R = R_w/r^*)$. Although these techniques have been successfully applied to a variety of transonic flow problems, they, unfortunately, have a common shortcoming: their inability to analyze nozzles having small normalized throat wall radii of curvature $R < 1$. For most rocket nozzles of current interest, $R \lesssim 1$, and it is generally believed that the expansion methods are inapplicable. It will be shown, however, that this limitation is due to the coordinate system em-

Received October 21, 1968; revision received March 5, 1969.

* President.
† Staff Scientist, Aerosciences Department.

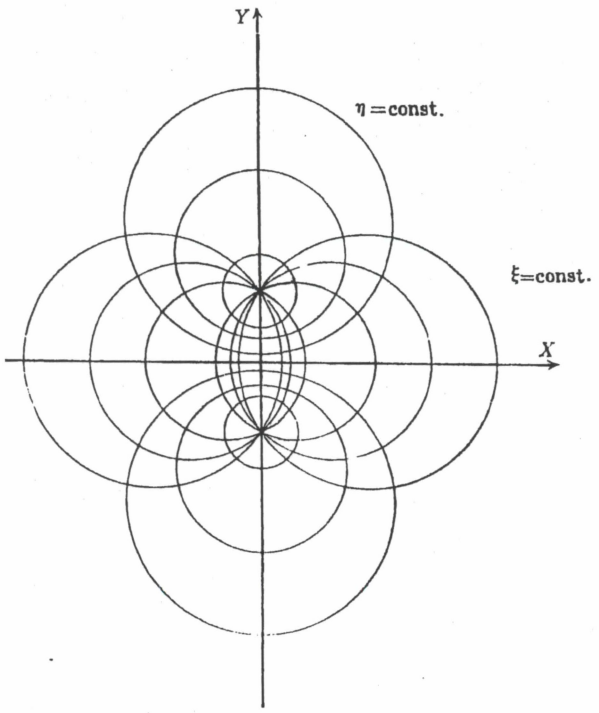

Fig. 1 Toroidal coordinates.

ployed in the analysis rather than to a fundamental limitation of the expansion method itself.

Hall[1] carried out a small perturbation transonic solution for irrotational, perfect gas flow, in cylindrical coordinates, by means of expansions in inverse powers of R, the normalized throat wall radius of curvature. His solution gives the normalized (with the sonic velocity) axial and radial velocity components in the form

$$u = 1 + \frac{u_1(r,z)}{R} + \frac{u_2(r,z)}{R^2} + \frac{u_3(r,z)}{R^3} + \dots \quad (1)$$

$$v = \left(\frac{\gamma+1}{2R}\right)^{1/2}\left[\frac{v_1(r,z)}{R} + \frac{v_2(r,z)}{R^2} + \frac{v_3(r,z)}{R^3} + \dots\right] \quad (2)$$

where $z = [2R/(\gamma+1)]^{1/2}x/r^*$ is the transformed normalized axial coordinate and $r = y/r^*$ is the normalized radial coordinate. In reviewing Hall's work, it was discovered that his published axisymmetric solution contained errors in the third-order terms (u_3,v_3) and the discharge coefficient. Since Hall's work is widely used in the field, the complete, corrected, third-order axisymmetric solution is given in the Appendix.

The expansion parameter $1/R$ in Eqs. (1) and (2) is introduced through the wall boundary condition, which requires the flow angle to be equal to the local wall slope at the boundary. The boundary is not a constant coordinate line in cylindrical coordinates and must be evaluated as a power series in $1/R$. Thus, the wall boundary condition is never exactly satisfied in cylindrical coordinates. In addition, the radial wall velocity v is proportional to the boundary slope, which can become large in the vicinity of the throat in nozzles having small ($R < 1$) normalized throat wall radius of curvature. It is reasonable to expect that the accuracy of the solution could be improved by seeking a solution in a coordinate system in which the axis and wall are both coordinate lines. In such a coordinate system, the boundary conditions are reduced to their simplest form and can be satisfied exactly. In addition, the normal coordinate lines are approximately streamlines and the normal velocity component is always small throughout the flowfield, being identically zero at both the wall and axis. For nozzles having circular arc throats, the optimum coordinate system would thus appear to be toroidal coordinates (Fig. 1), since in this coordinate system the axis is represented by the line $\eta = 0$ and the nozzle wall is represented by the line $\eta = \eta_w$ (a constant).

The relationship between the cylindrical coordinates x, y and the toroidal coordinates ξ, η is given by

$$y/r^* = (1+2R)^{1/2}\sinh\eta/(\cosh\eta + \cos\xi) \quad (3)$$

$$x/r^* = (1+2R)^{1/2}\sin\xi/(\cosh\eta + \cos\xi) \quad (4)$$

where $-\pi \leq \xi \leq \pi$, $-\infty \leq \eta \leq \infty$, and the throat plane is at $\xi = 0$. The wall contour in toroidal coordinates, in terms of the normalized wall radius of curvature, is

$$\eta_w = \frac{1}{2}\ln\frac{1+(1+2R)^{1/2}/(1+R)}{1-(1+2R)^{1/2}/(1+R)} \quad (5)$$

which can be expanded as

$$\eta_w = \frac{(2)^{1/2}}{(1+R)^{1/2}}\left[1 + \frac{0.4166}{(1+R)} + \frac{0.2688}{(1+R)^2} + \frac{0.1976}{(1+R)^3} + \frac{0.1556}{(1+R)^4} + \frac{0.1280}{(1+R)^5} + \dots\right] \quad (6)$$

convergent for all $R > 0$. Thus, utilizing the wall coordinate in toroidal coordinates as a normalization quantity introduces the perturbation parameter $1/(R+1)$ into the solution, whereas in cylindrical coordinates the perturbation parameter appears as $1/R$ through the wall boundary condition. The perturbation parameter $1/(R+1)$ remains less than 1 for all normalized wall radii of curvature. Thus, the convergence properties of an expansion solution obtained in toroidal coordinates should be superior to that given by Hall for cylindrical coordinates. Since the two solutions must be identical in the limit of large radii of curvature, one can transform Hall's results from an expansion in $1/R$ to an expansion in $1/(R+1)$, which is the form one would obtain (to the specified order) by transforming the solution in toroidal coordinates to Cartesian coordinates. Thus, the solution given by Eqs. (1) and (2) and the solution expressed as

$$u = 1 + \frac{u_1(r,z)}{(R+1)} + \frac{1}{(R+1)^2}[u_1(r,z) + u_2(r,z)] + \frac{1}{(R+1)^3}[u_1(r,z) + 2u_2(r,z) + u_3(r,z)] + \dots \quad (7)$$

$$v = \left[\frac{\gamma+1}{2(R+1)}\right]^{1/2}\left\{\frac{v_1(r,z)}{R+1} + \frac{1}{(R+1)^2}\times\left[\frac{3}{2}v_1(r,z) + v_2(r,z)\right] + \frac{1}{(R+1)^3}\times\left[\frac{15}{8}v_1(r,z) + \frac{5}{2}v_2(r,z) + v_3(r,z)\right] + \dots\right\} \quad (8)$$

are equivalent, the error being of order $1/R^4$ in each, for the limit of large R. The preceding solution is expected to be useful for all R since the η_w expansion is convergent for all R whereas Hall's solution would appear to be divergent for $R < 1$, since one can transform an expansion of the form $1/(R+1)$ into an expansion of the form $1/R$ only for $R > 1$. One could obtain the aforementioned solutions completely in toroidal coordin-

Table 1 Comparison between theory and experiment

	Theory	Experiment
C_D	0.982	0.985
u_0	0.816	0.827
u_w	1.24	1.31
x_0^*	0.199	0.206
r_0^*	0.598	0.633
x_w^*	−0.150	−0.136

ates either by solving the equations of motion directly in toroidal coordinates or expanding the coordinate transformation [Eqs. (3)and (4)] in terms of $1/(R + 1)$, substituting into Eqs. (7) and (8), and collecting like powers of $1/(R + 1)$.

In order to demonstrate the properties of the solution in toroidal coordinate form, the throat velocity at the axis u_0 and wall u_w, and the discharge coefficient C_D have been computed using both the Hall solution and the present solution. The equations for the throat wall and axis velocities and the nozzle discharge coefficient are

$$u_0 = 1 - \frac{1}{4R} + \frac{10\gamma + 57}{288R^2} - \frac{2708\,\gamma^2 + 7839\gamma + 14211}{82944R^3} \tag{9}$$

$$= 1 - \frac{1}{4(1 + R)} + \frac{10\gamma - 15}{288(1 + R)^2} - \frac{2708\gamma^2 + 2079\gamma + 2115}{82944(1 + R)^3} \tag{10}$$

$$u_w = 1 + \frac{1}{4R} - \frac{(14\gamma + 15)}{288R^2} + \frac{2364\gamma^2 + 4149\gamma + 2241}{82944R^3} \tag{11}$$

$$= 1 + \frac{1}{4(1 + R)} - \frac{(14\gamma - 57)}{288(1 + R)^2} + \frac{2364\gamma^2 - 3915\gamma + 14337}{82944(1 + R)^3} \tag{12}$$

$$C_D = 1 - \frac{\gamma + 1}{R^2}\left[\frac{1}{96} - \frac{8\gamma + 21}{2304R} + \frac{754\gamma^2 + 2123\gamma + 2553}{276480R^2}\right] \tag{13}$$

$$C_D = 1 - \frac{\gamma + 1}{(1 + R)^2}\left[\frac{1}{96} - \frac{(8\gamma - 27)}{2304(1 + R)} + \frac{754\gamma^2 - 757\gamma + 3633}{276480(1 + R)^2}\right] \tag{14}$$

The results of calculations for $\gamma = 1.4$ are shown in Figs. 2 and 3 as plots of the first, second, and third-order values of u_0, u_w, and C_D vs the expansion parameter $1/(1 + R)$. The marked improvement in solution behavior is vividly demonstrated. It can be seen that Hall's solution seriously deteriorates for R less than 1.5 and becomes divergent in an oscillatory manner for R less than 1, whereas the present solution remains

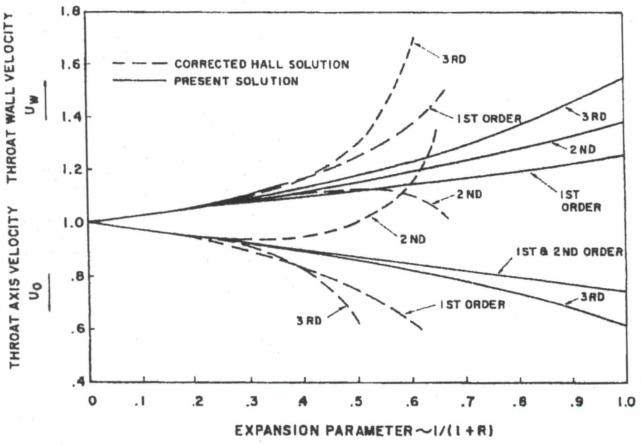

Fig. 2 Comparison of Hall's solution to the present results for the throat wall and axis velocities.

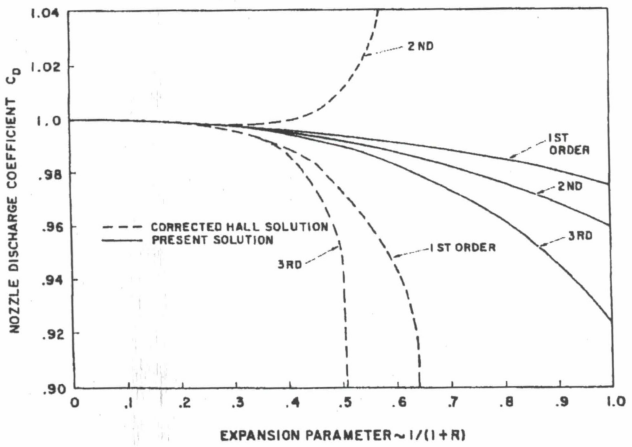

Fig. 3 Comparison of Hall's solution to the present results for the discharge coefficient.

well behaved for all R and does not diverge in an oscillatory manner.

It should also be noted that for nozzles having normalized wall radii of curvature in the neighborhood of unity, the sharp drop in the nozzle discharge coefficient predicted by Hall's third-order analysis appears to be associated with the convergence properties of Hall's solution. The present analysis predicts that the nozzle discharge coefficient remains reasonably high for all nozzles. It is also interesting to note that the current solution approaches physically reasonable finite limits for the throat flow properties as R goes to zero. The solution for $R = 0$ represents the flow through an axisymmetric sharp edged orifice, a problem which has not previously been solved.

The final test of any theoretical method is, of course, how well it predicts the actual phenomena under consideration, as evidenced by a comparison with experimental data. Cuffel et al.[7] have compared the results obtained with the present method to experimental data for a nozzle with $R = 0.625$. The predicted and measured sonic line parameters are summarized in Table 1. The throat axis, wall velocities, and nozzle discharge coefficient were computed from Eqs. (10, 12, and 14), respectively, whereas the axis sonic point displacement x_0^*, the radial distance to the throat sonic point crossing r_0^*, and wall sonic point displacement x_w^*, were computed from

$$x_0^* = \left[\frac{\gamma + 1}{32(R + 1)}\right]^{1/2}\left[1 - \frac{4\gamma - 15}{72(R + 1)} + \frac{824\gamma^2 + 540\gamma + 1818}{20736(R + 1)^2} + \ldots\right]r_t \tag{15}$$

$$r_0^* = (2)^{-1/2}\left[1 + \frac{4\gamma + 3}{72(R + 1)} + \frac{-1332\gamma^2 + 93\gamma + 657}{41472(R + 1)^2} + \ldots\right]r_t \tag{16}$$

$$x_w^* = -\left[\frac{\gamma + 1}{32(R + 1)}\right]^{1/2}\left[1 - \frac{20\gamma - 3}{72(R + 1)} + \frac{4440\gamma^2 - 1404\gamma - 1998}{20736(R + 1)^2} - \ldots\right]r_t \tag{17}$$

The excellent agreement between theory and experiment for such a small throat wall radius of curvature nozzle ($R = 0.625$) confirms that the present transonic expansion analysis is applicable to axisymmetric nozzles having circular arc throats with $R < 1$. Transformation of Hall's cylindrical results into other coordinate systems in which both the axis and wall are natural coordinate lines should lead to similar improvements in the prediction of transonic flow properties in nozzles having other wall shapes.

Appendix

It was discovered that Hall's[1] published axisymmetric solution contained errors in the third-order terms and discharge coefficient. The authors have rederived the solution and performed numerical cross checks to verify the results. The complete, corrected, third-order axisymmetric solution for the velocity components and discharge coefficient is given in the following:

$$u_1 = \tfrac{1}{2}r^2 - \tfrac{1}{4} + z \tag{A1}$$

$$v_1 = \tfrac{1}{4}r^3 - \tfrac{1}{4}r + rz \tag{A2}$$

$$u_2 = \frac{2\gamma+9}{24}r^4 - \frac{4\gamma+15}{24}r^2 + \frac{10\gamma+57}{288} + z\left(r^2 - \tfrac{5}{8}\right) - \frac{2\gamma-3}{6}z^2 \tag{A3}$$

$$v_2 = \frac{\gamma+3}{9}r^5 - \frac{20\gamma+63}{96}r^3 + \frac{28\gamma+93}{288}r + z\left(\frac{2\gamma+9}{6}r^3 - \frac{4\gamma+15}{12}r\right) + rz^2 \tag{A4}$$

$$u_3 = \frac{556\gamma^2+1737\gamma+3069}{10368}r_6 - \frac{388\gamma^2+1161\gamma+1881}{2304}r^4 + \frac{304\gamma^2+831\gamma+1242}{1728}r^2 - \frac{2708\gamma^2+7839\gamma+14211}{82944} + z\left[\frac{52\gamma^2+51\gamma+327}{384}r^4 - \frac{52\gamma^2+75\gamma+279}{192}r^2 + \frac{92\gamma^2+180\gamma+639}{1152}\right] + z^2\left[-\frac{7\gamma-3}{8}r^2 + \frac{13\gamma-27}{48}\right] + \frac{4\gamma^2-57\gamma+27}{144}z^3 \tag{A5}$$

$$v_3 = \frac{6836\gamma^2+23031\gamma+30627}{82944}r^7 - \frac{3380\gamma^2+11391\gamma+15291}{13824}r_5 + \frac{3424\gamma^2+11271\gamma+15228}{13824}r^3 - \frac{7100\gamma^2+22311\gamma+30249}{82944}r + z\left[\frac{556\gamma^2+1737\gamma+3069}{1728}r^5 - \frac{388\gamma^2+1161\gamma+1181}{576}r^3 + \frac{304\gamma^2+831\gamma+1242}{864}r\right] + z^2\left[\frac{52\gamma^2+51\gamma+327}{192}r^3 - \frac{52\gamma^2+75\gamma+279}{192}r\right] - z^3\left[\frac{7\gamma-3}{12}r\right] \tag{A6}$$

The ratio of the mass flow through the nozzle to the "one-dimensional" mass flow (discharge coefficient) is given by

$$C_D = 2\int_0^1 \left(\frac{\rho u}{\rho^* a^*}\right)_{z=0} r\,dr \tag{A7}$$

which, when integrated, yields Eq. (13).

References

[1] Hall, I. M., "Transonic Flow in Two-Dimensional and Axially-Symmetric Nozzles," *Quarterly Journal of Mechanics and Applied Mechanics*, Vol. XV, Pt. 4, 1962, pp. 487–508.

[2] Sauer, R., "General Characteristics of the Flow Through Nozzles at Near Critical Speeds," TM1147, June 1967, NACA.

[3] Oswatitsch, K. and Rothstein, W., "Flow Pattern in a Converging-Diverging Nozzle," TM1215, March 1949, NACA.

[4] Mendelson, R. S., "A General Transonic Flow Analysis for Axially-Symmetric Rocket Nozzles," TR HSM-R037, Feb. 1964, Chrysler Corp. Space Division, Huntsville, Ala.

[5] Sims, J. L., "Calculation of Transonic Flow," TMX-53081, Oct. 1964, NASA.

[6] Kliegel, J. R. and Quan, V., "Convergent-Divergent Nozzle Flows," Rept. 02874-6002-R000, Dec. 1966, TRW Systems, Redondo Beach, Calif.

[7] Cuffel, R. F., Back, L. H., and Massier, P. F., "The Transonic Flowfield in a Supersonic Nozzle with Small Throat Radius of Curvature," *AIAA Journal*, Vol. 7, No. 7, July 1969, pp. 1364–1366.

Two Formulations for Optimization Problems with State-Variable Inequality Constraints

G. J. LASTMAN*

University of Waterloo, Waterloo, Ontario, Canada

THE following optimization problem is to be considered: minimize the functional

$$I_1 = G[X(t_1),t_1] + \int_{t_0}^{t_1} Q[X(t),U(t),t]dt$$

subject to

$$dX(t)/dt = \dot{X}(t) = F[X(t),U(t),t]; \quad t_0 \le t \le t_1$$

$$X(t_0),\ t_0 \text{ known constants}; \quad L[X(t_1),t_1] = 0$$

$$S[X(t),t] \le 0; \quad t_0 \le t \le t_1$$

where $X = (X_1,X_2,\ldots,X_n)^T$, $U = (U_1,U_2,\ldots,U_m)^T$, $F = (F_1,F_2,\ldots,F_n)^T$, $L = (L_1,L_2,\ldots,L_l)^T$. It is assumed that only one state-variable inequality constraint is present and that the trajectory is on the constraint boundary $S = 0$ only for $t_\epsilon \le t \le t_\lambda$. The state-variable constraint $S[X(t),t]$ is assumed to be a qth-order constraint; i.e., S and its first $q-1$ derivatives with respect to t do not explicitly contain the control U, but the qth derivative of S does contain U, $d^qS/dt^q = C[X(t),U(t),t]$.

Following Bryson et al.,[1] the following conditions must hold at $t = t_\epsilon$:

$$S[X(t_\epsilon),t_\epsilon] = 0$$

$$d^jS[X(t_\epsilon),t_\epsilon]/dt^j = S^{(j)}[X(t_\epsilon),t_\epsilon] = 0$$

$$j = 1,2,\ldots,q-1$$

For $t_\epsilon \le t \le t_\lambda$ the control is computed from $S^{(q)} = C[X(t),U(t),t] = 0$. These tangency conditions insure that the extremal trajectory will not violate the constraint $S \le 0$.

In order to obtain necessary conditions for an extremal trajectory an augmented functional I_2 is formed

$$I_2 = R[X(t_1),\nu,t_1] + \xi^T W[X(t_\epsilon),t_\epsilon] + \int_{t_0}^{t_1} (H - P^T\dot{X})dt$$

where

$$R[X(t_1),\nu,t_1] = G[X(t_1),t_1] + \nu^T L[X(t_1),t_1]$$

$$W_i[X(t_\epsilon),t_\epsilon] = S^{(i-1)}[X(t_\epsilon),t_\epsilon]; \quad 1 \le i \le q \ (S^{(0)} = S)$$

$$W = (W_1,W_2,\ldots,W_q)^T$$

Received September 23, 1968; revision received March 7, 1969. Supported in part by N.R.C. (Canada) under Grant A-4753.

* Assistant Professor, Department of Applied Mathematics.